Journal of the Serbian Chemical Society
JSCS-info@shd.org.rs • www.shd.org.rs/JSCS

J. Serb. Chem. Soc. 90 (11) 1331–1352 (2025)
JSCS–5457

Original scientific paper
Published 13 November 2025

Optimisation of the controlled release of valsartan *via* cellulose acetate butyrate and poly(butylene succinate) microspheres: Influence of formulation conditions

AISSA BOUHARAOUA[1], HAOUARIA MERINE[1] and YOUSSEF RAMLI[2]*

[1]*Laboratory of Macromolecular Physical and Organic Chemistry, Faculty of Exact Sciences, University of Djillali Liabes, Sidi Bel-Abbes, Algeria and* [2]*Laboratory of Medicinal Chemistry, Drug Sciences Research Center, Faculty of Medicine and Pharmacy, Mohammed V University, Rabat, Morocco*

(Received 21 May, revised 15 July, accepted 10 September 2025)

Abstract: This study investigates the formulation of valsartan-loaded cellulose acetate butyrate (CAB) microspheres, prepared *via* solvent evaporation microencapsulation, to evaluate their *in vitro* release behavior and the influence of formulation parameters. The study examined the effects of stirring speed, stabilizers and matrix materials on particle size and drug release. Increasing stirring speed reduced particle size but also led to higher valsartan loss, reducing encapsulation efficiency. Using the surfactant polylactic acid resulted in smooth, spherical and porous microspheres that enhanced controlled release. In contrast, using Tween 80 led to irregular particles with rough surfaces and larger pores that accelerated drug release. Including poly(butylene succinate) in the matrix resulted in smaller microparticles forming and a significantly higher rate of valsartan release. These findings emphasize the importance of optimizing formulation parameters and excipients to control drug release characteristics and enhance drug delivery system performance.

Keywords: valsartan; microencapsulation; polymer carriers; formulation conditions; controlled release.

INTRODUCTION

Valsartan (Vals), chemically known as (2*S*)-3-methyl-2-[pentanoyl-[[4-[2--(2*H*-tetrazol-5-yl)phenyl]phenyl]methyl]amino]butanoic acid, is a potent and selective competitive antagonist of the AT1 angiotensin II receptors and is widely prescribed for the treatment of hypertension (Scheme.1).[1,2]

By inhibiting angiotensin II, it causes vasodilatation, reduces blood pressure and improves blood flow.[3,4] As a tetrazole derivative, valsartan contains acidic

* Corresponding author. E-mail: merine_houaria@yahoo.fr
https://doi.org/10.2298/JSC250521068B

(pK_a 4.73) and carboxylic (pK_a 3.9) groups that contribute to its pH-dependent solubility. Specifically, its solubility increases by a factor of 1000 when the pH is shifted from 4 to 6. The compound exhibits complete and rapid dissolution in vitro at pH 5.0 or higher, suggesting that its rate of absorption is influenced by the pH of the gastrointestinal tract.[5]

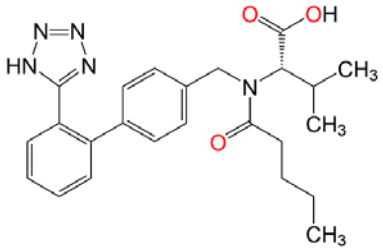

Scheme 1. Chemical structure of valsartan.

Valsartan is poorly soluble in the upper gastrointestinal tract, where most of its absorption occurs. This poor solubility limits absorption, leading to low oral bioavailability (approximately 23 %),[6] despite rapid uptake. To overcome this issue, sustained-release formulations are required. Microencapsulation is being explored as an effective method of controlling drug release and improving therapeutic efficacy.[7]

Solvent evaporation microencapsulation is a widely recognised technique for the production of microparticles, valued for its simplicity of manufacture while maintaining drug efficacy. In studies on valsartan, the preparation of valsartan-loaded microspheres using different matrices such as poly-ε-caprolactone (PCL) and polylactic acid (PLA) showed that PCL provided a more controlled and gradual release of valsartan compared to PLA when tested in vitro in a phosphate-buffered saline solution at pH 6.8. Furthermore, analysis of various factors affecing encapsulation – such as surfactant concentration, PLA amount, aqueous phase volume and stirring speed-showed that increasing surfactant concentration and aqueous phase volume negatively affected the encapsulation rate of valsartan, leading to a decrease in encapsulation efficiency as these parameters were increased.[2]

Previous studies have mainly focused on the formation of inclusion complexes with cyclodextrins,[8,9] the development of solid dispersions using hydrophilic carriers[1,10] and encapsulation within lipids like lecithin and cholesterol.[6,11] These strategies aim to improve the solubility and bioavailability of poorly water-soluble drugs. However, research specifically targeting the encapsulation of valsartan in polymeric matrices remains relatively limited, despite the potential benefits in terms of controlled release and stability. However, some studies have made significant contributions in this area, particularly those investigating the encapsulation of valsartan in gelatin and hydroxypropyl methylcellulose (HPMC)

by spray drying,[12] using gelation techniques with sodium alginate and HPMC,[13] and nanoprecipitation for Eudragit L100.[14] These efforts highlight the growing interest in polymer-based delivery systems for valsartan, although further investigation is needed to optimise these techniques for clinical applications.

In this study, two carrier systems were used to develop rapid release solid formulations: the biodegradable and non-toxic polymeric matrices CAB and PBS, a biodegradable aliphatic polyester. Cellulose acetate has been used extensively in temporary surgical materials (such as sutures, plates and screws) and as a matrix for encapsulating and releasing therapeutic agents in the human body.[15] PBS, with properties similar to polyolefins, offers advantages such as heat resistance and balanced mechanical properties, making it suitable for a wide range of applications.[16]

Our research group recently investigated the preparation of hydrochlorothiazide (HCTZ)-loaded microspheres using different matrices, such as ethylcellulose, PCL, β-cyclodextrin (β-CD) and poly(methyl methacrylate) (PMMA), synthesised in different fractions, to analyse their influence on encapsulation efficiency and drug release kinetics.[17] In addition, Badis *et al.*[18] continued the study of allopurinol encapsulation using different matrices, including EC, HPMC, β-CD and PCL, using the solvent evaporation method for extended release of this drug. As part of our efforts to develop new drug formulations that allow a gradual release of the active ingredient and overcome the limitations of traditional pharmaceutical forms, in particular to reduce the frequency of administration, we investigated the encapsulation of valsartan using two matrices (CAB and PBS), also using the solvent evaporation method for extended release. This study also focused on characterising the interaction between valsartan and the matrix by evaluating the influence of several factors such as stirring speed, stabiliser effect and the ratio of the dispersed phase to the continuous phase. Micro- and nano-sized particles were characterised using spectroscopic techniques, including Fourier transform infrared (FTIR) spectroscopy and powder X-ray diffraction (PXRD), to study their dissolution behaviour. The main objective of this study was also to evaluate the impact of these factors on the encapsulation efficiency and drug release kinetics in the intestinal tract.

MATERIALS AND METHODS

Chemicals

Valsartan (molar mass: 435.518±0.0231 g mol^{-1}) was generously provided by the Therapeutic Chemistry Laboratory at the Faculty of Medicine and Pharmacy, Mohamed V University in Rabat, Morocco. The micro-encapsulation of solid microspheres was achieved using the solvent evaporation technique, utilizing our synthesized PBS and CAB as matrices, with valsartan as the active agent. CAB, with a viscosity of 0.1 Pa s for a 5 mass % solution in a toluene/ethanol mixture (ϕr = 4:1), was sourced from Merck (India), while polyvinyl alcohol (PVA, 87–90 % hydrolysed, molar mass 30000–70000) and Tween 80 were purchased from

Sigma–Aldrich. Dichloromethane (DCM >98 % purity) was used as the internal phase. A phosphate buffer solution at pH 7.4 was prepared by mixing 250 mL of 0.2 M monobasic potassium phosphate (KH_2PO_4) solution with 195.5 mL of 0.1 M sodium hydroxide solution and adjusting the final volume to 1 L with deionized water.

Synthesis and characterization of poly(butylene succinate) (PBS)

The synthesis of PBS was successfully carried out using ring-opening polymerization. A mixture of butan-1,4-diol (0.12 mol) and succinic acid (0.10 mol) was reacted in the presence of 1–2 % titanium isopropoxide as a catalyst. The reaction was refluxed for 2 h at 180 °C with vigorous stirring under a nitrogen atmosphere. To purify the obtained polymer and remove any residual monomers, the product was heated at 200 °C under reduced pressure (maximum of 10^{-3} mm Hg) for three hours.[18,19]

The white PBS powder was characterized; IR, $\bar{\nu}$ (cm^{-1}): 1710, C=O (ester); 2920–2940 (CH_2); 1100–1200 (ester C–O–C); 1310–1330 (C–H); 3429–3552 (terminal O–H). ^{1}H-NMR spectra, Scheme 2: $\delta_H(CDCl_3)$, ppm: 1.65 (CH_2(a)); 1.55 (CH_2(a')); 2.55 (CH_2(c)); 4.05 (CH_2(b)); 3.55 (CH_2(d)). ^{13}C-NMR**,** ppm: 25 (CH_2(a)); 25 (CH_2(a')); 29 (CH_2(c)); 64 (CH_2(b)); 62 (CH_2(d)); 172 (CO ester).

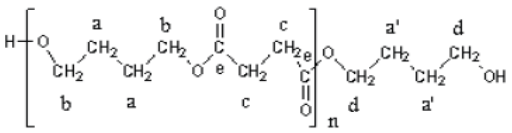

Scheme 2. Chemical structure of poly(butylene succinate) (PBS).

Preparation of solid dispersions

To prepare solid dispersions of valsartan, CAB polymer was combined with valsartan by solvent evaporation in a 2:1 weight ratio (polymer corresponding to 50 % valsartan by weight relative to the polymer). First, valsartan and the polymer were dissolved in dichloromethane (DCM), a water-immiscible organic solvent, in amounts of 66 or 33 g, as required. This organic solution was then poured into 250 g of deionised water, which served as the external phase, containing 1 % PVA or Tween (1 % by mass in water, as specified). Emulsification of the organic phase with the aqueous phase was achieved by mechanical stirring at two speeds (800 or 1200 rpm) in a 600 mL glass reactor (diameter = 80 mm) using a four-bladed turbine impeller (blade length = 50 mm, width = 8 mm; IKA RW20 digital, UK). Valsartan microencapsulation was completed after 3 h at room temperature to allow time for solvent evaporation. The resulting microparticles were collected by vacuum filtration, rinsed several times with deionised water and dried in a desiccator with $CaCl_2$ for at least 48 h. The initial composition of the different microsphere formulations is shown in Table I.

Microsphere characteristics

During the manufacture of microsphere formulations, the drug and polymer may come into close contact, potentially impacting the drug's stability. The evaluation of drug–polymer interactions is essential for the selection of a suitable polymer. Various methods have been used to evaluate the compatibility between valsartan and specific polymers.

Fourier transform infrared spectroscopy (FTIR)

The FTIR spectra of the drug, polymers and microparticles in powdered form were obtained using an Alpha Bruker IR spectrometer, covering the wavelength range of 400 to 4000 cm^{-1}.

TABLE I. Processing conditions for the formulated microspheres

Code	Composition	N / rpm	Emulsifier nature	DCM volume, cm^3
L1	CAB/Vals	800	PVA	50
L2	CAB/Vals	1200	PVA	50
L3	CAB/Vals	800	TWEEN	50
L4	CAB/Vals	1200	TWEEN	50
L5	CAB/Vals	800	PVA	25
L6	CAB/Vals	1200	PVA	25
L7	CAB/PBS/Vals	800	PVA	50
L8	CAB/PBS/Vals	1200	PVA	50

Powder X-ray diffraction (XRD)

XRD patterns of the pure drug, carriers, and microsphere formulations were captured using a Rigaku MiniFlex 600 (MiniFlex acquisition system, λ = 1.541 Å) over a 2θ range from 5 to 70°, and analyzed for comparative purposes.

Particle size analysis

The average diameters and size distribution of the microspheres were determined using optical microscopy (Optika 4083.B1), by counting over 500 microparticles for each preparation. The particle size distribution was calculated from various equations.[20,21] The calculations include the number mean diameter d_{10}, the surface mean diameter d_{32}, the weight mean diameter d_{43} and the size distribution δ. The average diameters and size distribution of the microspheres were assessed using two complementary techniques. Additionally, for formulations prepared at a stirring speed of 1200 rpm (L2, L4, L6 and L8), particle diameters were determined using a Zetasizer Nano ZS (Malvern Instruments, UK). This instrument operates based on dynamic light scattering (DLS), which estimates the hydrodynamic size of particles in suspension by analyzing fluctuations in the intensity of scattered light resulting from Brownian motion:

$$d_{10} = \Sigma n_i d_i / \Sigma n_i \quad (1)$$

$$d_{32} = \Sigma n_i d_i^3 / \Sigma n_i d_i^2 \quad (2)$$

$$d_{43} = \Sigma n_i d_i^4 / \Sigma n_i d_i^3 \quad (3)$$

$$\delta = d_{32}/d_{10} \quad (4)$$

Scanning electron microscopy of microparticles

The surface characteristics and morphology of valsartan microspheres were examined in detail using a scanning electron microscope (Hitachi TM 1000).

Determination of drug loading and microparticle yield

The valsartan content of the microspheres was assessed by extraction of the drug in absolute ethanol followed by spectrophotometric measurement at 251 nm (ε = 13681 L mol^{-1} cm^{-1}) using a UV spectrophotometer (model Shimadzu UV-2401). For each test, 40 mg of microparticles (prepared with CAB or CAB/PBS mixture, as appropriate) were dispersed in 10 mL of absolute ethanol in a sealed vial for 3 h. After appropriate dilution, the resulting solution was analysed for valsartan content by UV–Vis spectroscopy. The actual drug loading (*DL*), the encapsulation efficiency (*EE*) and yield (*PY*) of microspheres were calculated using the following equations:

$$DL = 100\frac{\text{Vals mass in microsphers}}{\text{mass of microsphers}} \quad (5)$$

$$EE = 100\frac{\text{Vals actual drug load}}{\text{Theoretical drug load}} \quad (6)$$

$$PY = 100\frac{\text{Microspheres recovered (practical mass)}}{\text{Mass of carrier and drug used in the formulation (theoretical mass)}} \quad (7)$$

In vitro *valsartan dissolution studies*

In vitro dissolution testing of valsartan from the prepared formulations was performed using a suitable glass dissolution reactor maintained in a water bath at 37±0.5 °C with a stirring speed of 500±1 rpm. Appropriate quantities of formulations containing 40 mg of valsartan were placed in 1000 mL glass flasks filled with 900 mL of simulated liquid at pH 7.4. At specified time intervals, 5 mL aliquots were removed from the dissolution medium and replaced with an equal volume of prewarmed (37±0.5 °C) fresh dissolution medium. Valsartan concentrations were measured using a Shimadzu UV-2401 UV–Vis spectrophotometer at the drug's maximum absorbance wavelength (λ(max) = 251 nm, ε = 13,105 $L \cdot mol^{-1} \cdot cm^{-1}$) in a phosphate buffer solution (pH 7.4) that simulated intestinal conditions. The amount of valsartan in each sample was determined spectroscopically and the corresponding drug release profiles were plotted, showing the cumulative percentage drug release (calculated from the total amount of Vals in each formulation) *versus* time. Each batch was tested in duplicate and the mean values were used for calculations. Two mathematical models, the Higuchi and Korsmeyer–Peppas equations, were used to analyse the drug transport mechanisms and predict the kinetics of drug release.[22-25]

RESULTS AND DISCUSSION

Microspheres characterizations

Excipients are an essential component in nearly all pharmaceutical dosage forms. The successful formulation of a stable and effective solid dosage form relies on selecting appropriate excipients, which are added to facilitate drug delivery and protect it from degradation.

In this study, eight microparticles were characterized in terms of shape, surface morphology, drug entrapment and size (mean diameter). The development of eight formulations loaded with valsartan using different polymers *via* solvent evaporation, with varying polymer proportions and experimental conditions, resulted in differences in particle size (mean diameter), surface morphology and drug entrapment. The results for drug loading (*DL*), percentage practical yield (*PY*), encapsulation efficiency (*EE*) and size distribution are presented in Table II.

The operating conditions of the microencapsulation process can influence the drug loading, the percentage of practical yield as well as the mean particle size and its distribution.[26,27]

Optical microscopy analysis of different samples prepared at a stirring speed of 800 rpm showed that the microparticle shapes were spherical with diameters

ranging from 69.7 to 3.5 μm. The particle size dispersion ranged from 1.65 for batch 3 to 1.24 for batch 7 (Fig. 1).

TABLE II. Results of the microencapsulation process for the prepared microspheres

Code	*DL* / %	*PY* / %	*EE* / %	d_{10} / μm	d_{32} / μm	d_{43} / μm	δ(PDI)
L1	33.18	84.96	84.58	45.7	56.2	62.3	1.36
L2	31.64	74.51	70.72		0.5		0.53
L3	23.75	59.77	42.58	48.9	69.7	80.7	1.65
L4	26.47	52	41.30		0.3		0.26
L5	30.182	55	49.76	5.3	6.3	7.0	1.31
L6	31.07	55	51.20		0.7		0.75
L7	32.03	50.09	48.20	3.0	3.5	3.8	1.24
L8	38.97	55.54	65		2.0		1

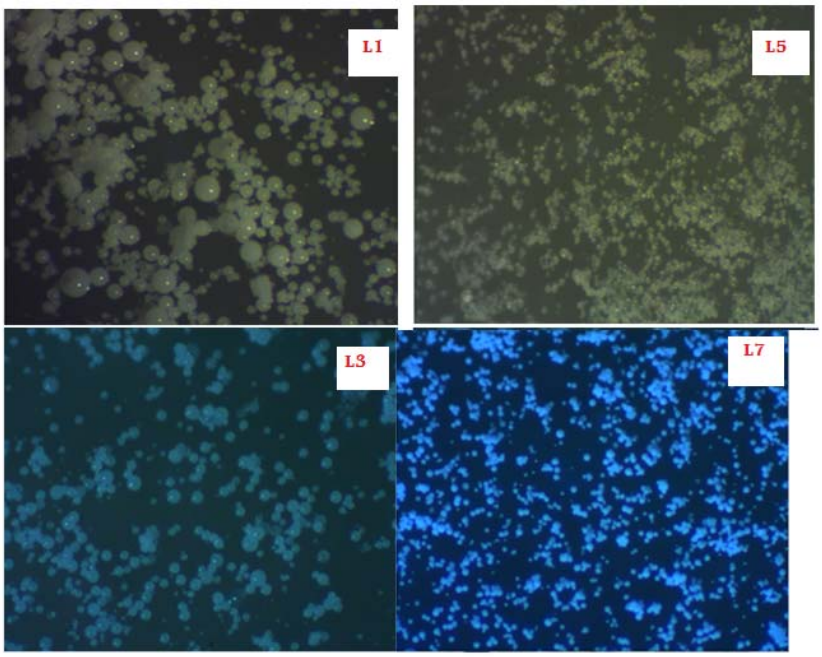

Fig. 1. Optical microscopy images of spherical valsartan-loaded CAB and PBS microparticles (L1, L3, L5 and L7), observed at 100× magnification.

For microparticles prepared at a speed of 1200 rpm (Lots: 2, 4, 6 and 8), the diameter study was carried out using a zetameter and dynamic light scattering (DLS). The rotation speed of 1200 rpm influenced the particle size and distribution, allowing optimal homogeneity in the formulation. The results showed that the microparticle diameter was in the range of 40 to 200 nm (Table II). This relatively small and well-defined size is particularly favourable for pharmaceutical

applications, ensuring better bioavailability and efficient diffusion of the drug into the target tissues. In addition, the narrow size distribution obtained is beneficial for controlling the release of the drug and maximising its therapeutic efficacy.[28]

The surface and morphology of the microspheres were also studied using scanning electron microscopy (SEM). The photographs of formulations 1 and 2, Fig. 2, show that the microparticles composed exclusively of cellulose butyrate acetate are individualised, spherical and have a rough surface.

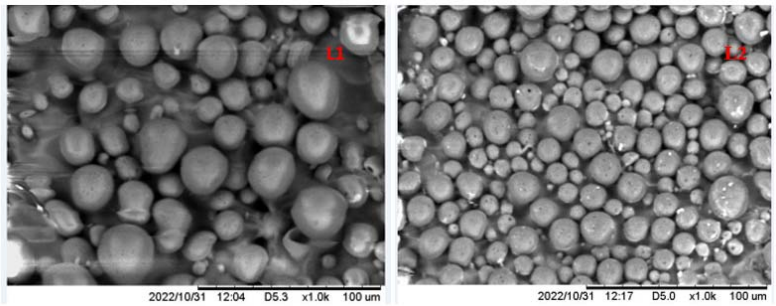

Fig. 2. SEM images showing the surface and morphology of Vals-loaded microspheres.

In all formulations the drug content ranged from 23.75 to 38.97 %, while the practical yield varied from 50.10 to 84.96 %. Formulation batch 3 had the lowest drug content while batch 8 had the highest. Furthermore, batch 1 had the highest yield while batch 7 had the lowest.

Various factors affect the content, yield, size and morphology of microparticles. In this study, we investigated how formulation parameters such as stirring speed, surfactant type, organic/aqueous phase fraction, as well as matrix composition and nature, have influence on microparticle characteristics.

Effect of stirring speed and shear

Agitation is a key parameter influencing microsphere size. The most common model for describing particle size variation with agitation is based on Kolmogorov's theory.[29]

In most studies, experimental results were in agreement with theoretical predictions. It has been observed that, under identical operating conditions, an increase in stirring speed affects the microsphere characteristics, in particular the size of the microspheres and the drug content.[18,30,31]

All formulations (L1–L8) exhibited well-defined, perfectly individualized spherical shapes (Fig. 1). The particle size distributions, determined by light microscopy and zeta analysis, showed a clear trend of decreasing particle size as the stirring speed increased from 800 to 1200 rpm. Specifically, the average particle size decreased from 56.2 μm in L1 to 0.5 μm in L2 and from 69.7 μm in L3 to 0.3

μm in L4. Furthermore, the size distribution (δ) improved from 1.52 to 1.31 under these conditions.

This reduction in particle size can be attributed to the higher energy input during emulsification at elevated stirring speeds (1200 rpm), which facilitates the efficient breakup of the organic phase into smaller, well-dispersed droplets.[32]

However, an inverse relationship was observed between stirring speed and drug loading. Formulations prepared with PVA as the emulsifier demonstrated this effect clearly. The drug loading, expressed as the percentage of the actual valsartan content in the microspheres relative to their mass, decreased from 33.18 in L1 to 31.64 % in L2 and from 49.76 % in L5 to 31.07 % in L6.

Many studies, including those by Mouffok *et al.*,[30] Badis *et al.*[18] and Merdoud *et al.*[31] have shown that higher stirring speeds typically result in smaller microparticle sizes and reduced encapsulation efficiency of the active ingredient. This effect is likely attributed to increased shear forces that interfere with the encapsulation process.

Effect of stabilising agents

Stabilizing agents are essential for maintaining emulsion stability, as they lower the interfacial tension between the continuous and dispersed phases. They also inhibit the coalescence and aggregation of emulsion droplets, especially in the early stages of solvent evaporation.[32,33]

The effect of PVA and Tween 80 surfactants on microspheres prepared under identical operating conditions (Vals ratio 1:2, stirring speed 800 rpm) is shown in Fig. 1. Microspheres stabilised with PVA (Fig. 1: L1) were spherical and smaller in size (d_{32} = 56.2 μm) compared to those stabilised with Tween 80 (d_{32} = 69.7 μm), which had a rough and porous surface (Fig. 1: L3).

Table II compares the effects of PVA and Tween 80 on key parameters including drug loading (DL), encapsulation efficiency (EE), yield, Sauter mean diameter (d_{32}) and size distribution (δ). Smaller microspheres were consistently obtained with PVA, consistent with results reported in the literature.[34]

PVA was more effective than Tween 80 in reducing the interfacial tension, thus limiting droplet coalescence during emulsification. Higher concentrations of PVA further improved drug loading and encapsulation efficiency while reducing mean particle size (d_{32}) and size distribution (δ). In particular, PVA achieved a higher encapsulation efficiency (*EE* = 84.58 % for L1) compared to Tween 80. This can be attributed to the properties of the polymer, the controlled stirring speed of 800 rpm and the smoother microsphere surfaces produced with PVA.

In contrast, microspheres prepared with Tween 80 exhibited significant surface porosity, resulting in significant loss of valsartan, which negatively affected both *DL* and *EE*. These observations are consistent with the findings of Mouffok

et al.,[30] who also highlighted the detrimental effect of surface porosity on drug encapsulation efficiency.

Effect of dispersed phase on continuous phase

The dispersed phase to continuous phase (D/C) ratio is a critical parameter in solvent evaporation microencapsulation as it significantly influences the properties of the resulting microparticles. Optimisation of this ratio is essential to achieve desired particle characteristics such as size, homogeneity, morphology and encapsulation efficiency. Experimental adjustments are often required to tailor the D/C ratio to the specific properties of the phases involved and the process objectives.[32,35,36]

A low D/C ratio generally results in better size homogeneity and smaller microparticles, as each droplet of dispersed phase contains less material and droplet formation is more controlled. In addition, low D/C ratios promote the formation of microspheres with smoother surfaces, probably due to the faster solidification rate. The higher water content in the continuous phase accelerates polymer precipitation, resulting in less porous microspheres.[36,37] Notably, a reduction in the D/C ratio was associated with a significant increase in encapsulation efficiency.[38]

Our results are consistent with previous findings. For example, a significant improvement in encapsulation efficiency (DL = 49.76 %) was observed in batch 5 (D/C ratio of 0.1) compared to batch 1 (DL = 33.18 % for D/C ratio of 0.2). As shown in Fig. 1, L5, with a lower D/C ratio, produced smaller microparticles (d_{32} = 6.3 μm) with a compact and well-formed surface. In contrast, L1, with a higher D/C ratio, produced larger microparticles (d_{32} = 56.2 μm) with a porous surface.

The influence of the D/C ratio was particularly evident in batches prepared at a stirring speed of 800 rpm, where differences in particle morphology and size were pronounced. However, for batches 2 and 6, prepared at a higher stirring speed of 1200 rpm, the effect of the D/C ratio was less pronounced as the increased stirring speed dominated the characteristics of the microparticles.

Impact of polymer properties

The properties of the polymer used play a critical role in determining encapsulation efficiency, particle size and drug release rate, as has been extensively discussed in the literature.[30,39–41] Two key parameters that influence the organic phase and consequently the encapsulation rate are polymer concentration and molar mass.

An increase in polymer mass or molar mass increases the viscosity of the organic phase, thereby limiting drug migration into the external aqueous phase.[42] This effect, which is attributed to faster precipitation of the polymer in the droplets, results in higher encapsulation efficiency.[39,43]

Similarly, polymer concentration and molar mass have a significant effect on particle size by modifying the viscosity of the organic phase, which in turn influences droplet rupture behaviour. Both theoretical and experimental studies[17,18,31,40,42,43] have shown that reducing the molar mass of the polymer at a constant solvent volume reduces the viscosity of the organic phase, facilitating the formation of smaller microparticles.

The inclusion of PBS in the formulations (L7 and 8) slightly improved drug entrapment compared to L1 and 2, which were prepared using the same solvent conditions, PVA concentrations and stirring speeds. L1 achieved a high yield of 84.58 %, reflecting minimal loss of microspheres during preparation and recovery. In contrast, L7 showed a lower yield of 49 %, which was influenced by polymer agglomeration and adhesion to the stirrer blades and beaker walls during microsphere formation. In addition, migration of small microparticles during filtration further reduced the yield for L7 (d_{32} = 3.5 μm).

The particle size distribution in batch 7 was narrower (δ = 1.24), probably due to the reduced viscosity in the dispersed medium caused by the lower molar mass of PBS. These results are consistent with previous studies reported in the literature.[17,18,31]

Microsphere spectroscopy

FTIR spectroscopy confirmed the actual presence of valsartan in the microspheres (Fig. 3) and highlighted the chemical stability of the drug. The FTIR spectra of the valsartan loaded microspheres were compared with those of pure valsartan and the CAB and PBS polymer matrices (Fig. 3).

The FTIR spectrum of pure valsartan (Fig.3a) is characterised by a broad band at 3444.86 cm^{-1}, corresponding to the stretching of the N–H bond as mentioned by Islas *et al*.[43] A band at 2961.67 cm^{-1} is observed, attributed to the extension of the –CH bond in the methyl group (CH_3). Two intense carbonyl bands are detected at 1730.38 and 1597.43 cm^{-1}, corresponding to the elongation of the C=O of the carboxyl group and the C=O of the amide function, respectively.

A band located at 755.83 cm^{-1} is associated with the out-of-plane deformations of the N–H bond in the primary amine. Finally, a band at 1409.56 cm^{-1} is observed, which is attributed to the stretching of the N=N bond.

The FTIR spectrum of CAB alone (Fig. 3b) showed a strong stretching vibration band at 1733.59 cm^{-1}, attributed to the C=O bond originating from the acetate and butyrate groups in the polymer. A series of characteristic absorption peaks for the CAB polymer were observed at 2961.82, 2935.20 and 2873.31 cm^{-1}, corresponding to the asymmetric and symmetric stretching vibrations of the CH_3 and CH_2 groups. The region between 1235 and 1050 cm^{-1} is associated with the stretching vibrations of the C–O bonds in the ester groups (acetate and butyrate).

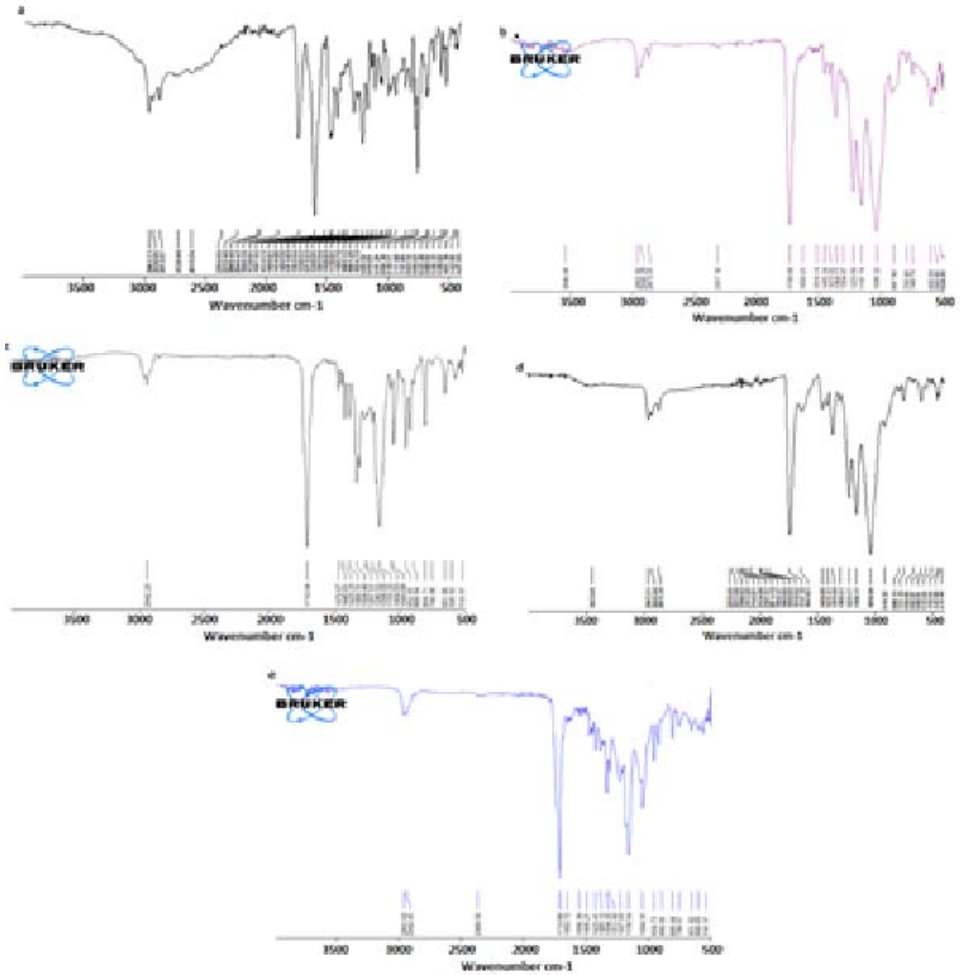

Fig. 3. FTIR patterns of: a) valsartan, b) CAB,(c) PBS, d) L1 and e) L7.

The infrared spectra of the microspheres (Fig. 3d) show characteristic bands similar to those of valsartan and CAB matrix, indicating the intact presence of the drug and polymer. In addition, a broad peak observed at the same positions as in the spectra of pure valsartan and CAB, without the appearance of new bands, suggests the absence of physical interaction between the drug and the polymers. The transmittance variations are explained by the concentration differences between the components.

The FTIR spectrum of batch 7 (Fig. 3e), derived from the combination of the two matrices CAB and PBS with valsartan, showed the characteristic stretching bands of the carbonyl group at 1711 cm^{-1} for the ester function of PBS and at 1650

cm^{-1} for valsartan. These results confirm the successful incorporation of both PBS (Fig. 3c) and valsartan (Fig. 3a) into the microspheres.

Finally, by comparing the IR-TF spectrum of pure valsartan with that of microspheres from batches 1 to 8, it is observed that the C=O band of the amide function (around 1597.43 cm^{-1}) has shifted to higher wave numbers. This shift can be attributed to the disruption of intermolecular and/or intramolecular hydrogen bonds in valsartan during its microencapsulation with CAB and PBS.[44]

The XRD spectrum of pure valsartan is shown in Fig. 4a. The XRD shows the absence of distinct peaks, indicating that valsartan is in amorphous form. Other studies such as Wang *et al.*[45] and Youn *et al.*,[46] have also observed an amorphous structure for pure valsartan.

Examining the XRD of the CAB polymer (Fig. 4b), it is noted that it does not show any crystalline peaks, suggesting an amorphous structure. This results in an amorphous combination when valsartan and CAB are physically mixed in microspheres (batches 1–6) as shown in the XRDs of batches 1, 3 and 5 (Fig. 4d–f).

In contrast, the X-ray diffractogram of the PBS polymer (Fig. 4c) shows a partially crystalline phase with two distinct peaks at 2θ equal to 19.67 and 22.72°, characterising a semi-crystalline structure.

A comparison of the X-ray diffraction patterns of valsartan, CAB and PBS with those of formulation L7 (see Fig. 4g) shows that the crystalline state of valsartan increases significantly in the solid dispersion while the characteristic peaks of PBS are maintained. Pure valsartan exhibited a broad amorphous halo in the 2θ range of 13.8–15.0°, but this was no longer observed in the L7 formulation. This suggests that valsartan underwent a partial structural reorganization into a semi-crystalline form.

Drug dissolution of valsartan

Valsartan, a tetrazole derivative, contains acidic (pK_a 4.73) and carboxylic groups (pK_a 3.9) that significantly affect its solubility, especially within the neutral pH range.[47] At physiological pH, it exists as undissociated acid, mono-anion or di-anion. Its solubility markedly increases between pH 4 and 6, favoring the anionic form but reducing lipophilicity, which in turn influences its gastrointestinal absorption. Dissolution becomes rapid and complete at pH 5.0 or higher.[48]

At 25 °C, valsartan's solubility in water is 0.18 g/L but rises substantially in buffered solutions, reaching 16.8 g/L in a phosphate buffer at pH 8.0. These properties are crucial for optimizing its formulation and therapeutic use.[3,5]

In this study, cellulose-based microparticles loaded with valsartan were developed and evaluated for controlled drug release. The release of the encapsulated drug was studied *in vivo* using simulated intestinal (colon) environment at 37 °C and compared with pure drug dissolution.

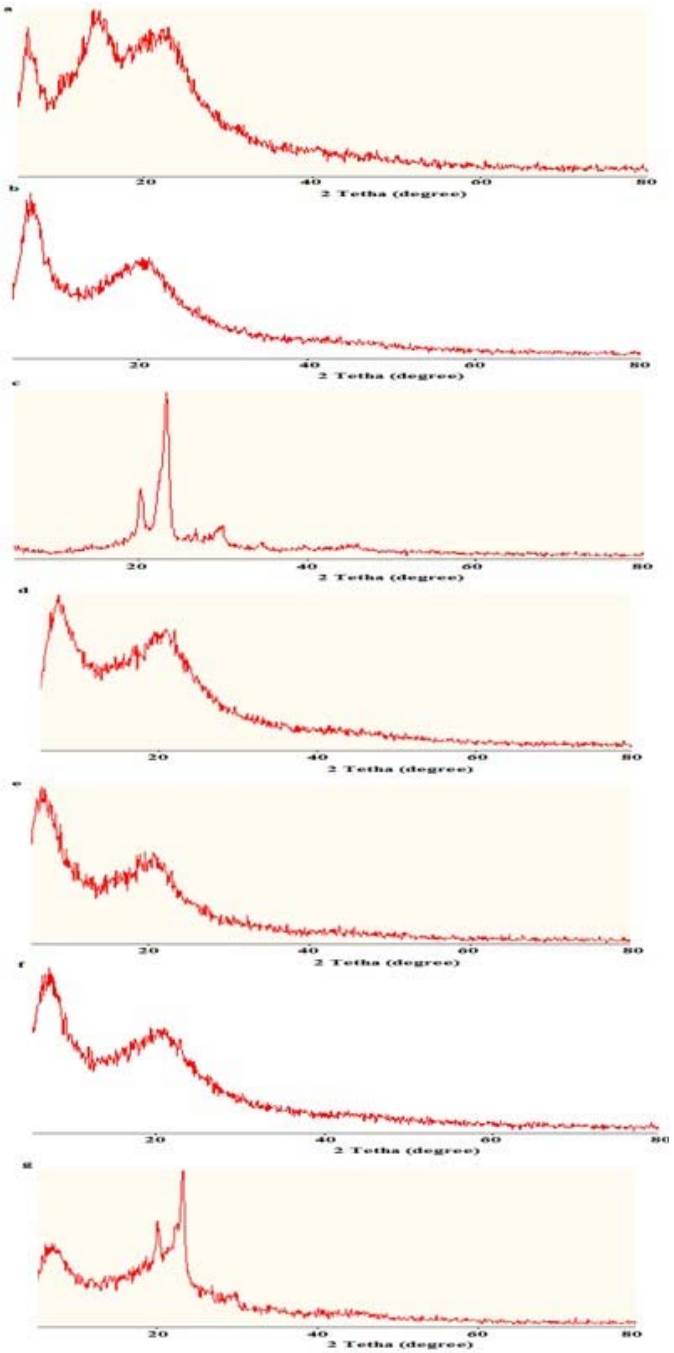

Fig. 4. XRD patterns of: a) valsartan, b) CAB, c) PBS, d) L1, e) L3, f) L5 and g) L7.

Various parameters were adjusted during the preparation process and their effect on drug release is analysed in this work. As highlighted earlier, the characteristics of the microparticles obtained, such as size, morphology and structure, were strongly influenced by the process variables and formulation conditions. These characteristics also influence the mass transfer mechanisms, potentially altering the release profiles.

The pure drug and the eight formulations were subjected to *in vitro* dissolution studies in simulated intestinal fluid (pH 7.4). Samples were collected at different time intervals, filtered and analysed at 251 nm. The dissolution profiles of the pure drug and the binary drug carrier system are shown in Figs. 5–7, and the *in vitro* release results of pure valsartan and all the formulations from L1 to F8 are shown in Table III. Furthermore, the release kinetics of Vals from these formulations were analyzed using the following models during the initial phase, up to 65 % drug release.

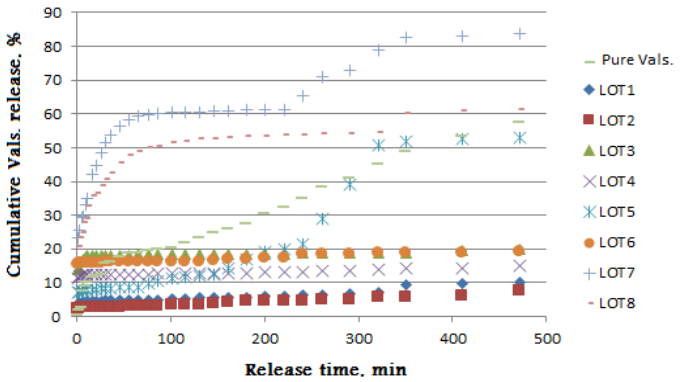

Fig. 5. Percent cumulative drug (Vals.) release *vs*. time in simulated intestinal fluid (pH 7.4).

For a clearer presentation of the results, discussion and to highlight the effects of the formulation parameters, we chose to directly and graphically compare the valsartan release profiles of the microparticle batches, varying each parameter individually.

It should be noted that CAB was used as the primary matrix in batches L1––L6. In addition, the effects of stirring speed, type of stabiliser and ratio of discontinuous to continuous phase were specifically investigated for CAB microspheres. Conversely, the influence of PBS polymer as a secondary matrix was evaluated in batches L7 and L8.

Firstly, the data presented in the table above indicate that valsartan exhibits a gradual but steady dissolution in the intestinal environment (pH 7). The release is initially limited but gradually increases, reaching about 60 % after 8 h.

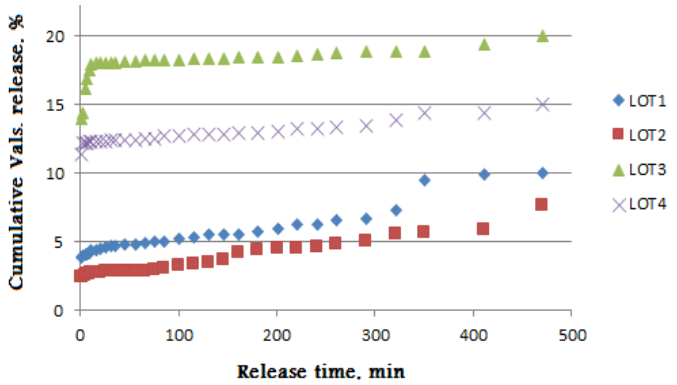

Fig. 6. Effect of stabilising agents in dissolution of valsartan from solid dispersions in simulated intestinal fluid (pH 7.4).

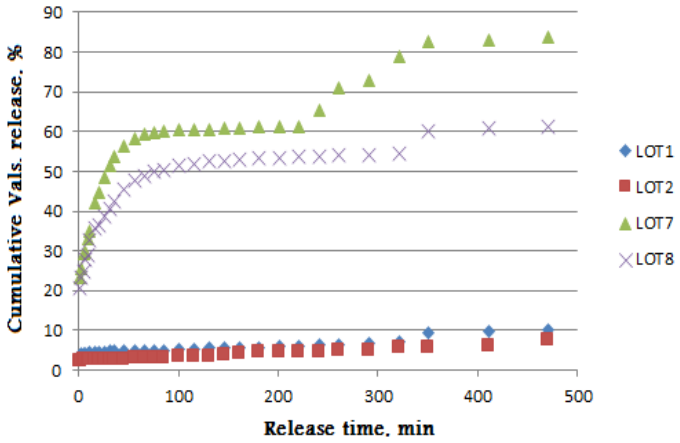

Fig. 7. Effect of PBS matrix in dissolution of valsartan from solid dispersions in simulated intestinal fluid (pH 7.4).

TABLE III. Percentage release data for Vals measured at 30 min and 1, 2 and 8 h

Code	Time			
	30 min	1 h	2 h	8 h
Pure Vals	15.70	18.72	22.50	57.40
L1	4.72	4.86	8.35	10.07
L2	2.80	2.86	3.35	7.64
L3	18.08	18.16	18.34	20.10
L4	12.36	12.44	12.81	15.10
L5	8.36	8.75	11.60	53.04
L6	16.01	16.05	16.20	19.32
L7	50.86	58.80	60.53	83.81
L8	40.61	47.65	51.85	61.17

The encapsulation of valsartan with cellulose acetate butyrate (CAB) significantly reduces its release in a medium at pH 7.4 (Fig. 5). This is likely due to the encapsulating effect of the polymer matrix and its hydrophobic nature, which limit water diffusion and drug release. This is supported by previous studies.[49] These properties slow down the disaggregation and diffusion of the drug while modifying its microstructural environment. These observations, which are consistent with the work of Merdoud *et al.*[31] who showed a slower release with CAB compared to ethyl cellulose (EC), suggest that CAB is a promising polymer for controlled release formulations.

The decrease in valsartan microparticle size results in a slight decrease in valsartan release, despite the literature linking rapid agitation during microencapsulation with improved release. This observation can be explained by several factors. Firstly, the agitation speeds used (800 and 1200 rpm) remain relatively high, producing microparticles of similar size, thus reducing significant differences in behaviour. Secondly, very small microparticles tend to agglomerate due to interparticle forces, reducing the effective surface area available for dissolution. In addition, the CAB (cellulose acetate butyrate) coating matrix could slow drug release by limiting diffusion from small particles due to physical and chemical barriers. These combined elements explain the slightly reduced release from very fine particles.

Fig. 6 shows that the cumulative release of microspheres prepared with Tween 80 (batches 3 and 4) was faster than that of those containing PVA (batches 1 and 2) due to their porosity and surface morphology (Fig. 6). These findings are consistent with those of Mouffok *et al.*,[30] who also emphasised the negative impact of surface porosity on drug release. Finally, the introduction of another matrix, such as low molecular weight PBS, also leads to a rapid release of valsartan, as observed in batches 7 and 8 compared to batches 1 and 2 (Fig. 7).

Release mechanisms and mathematical analysis

Mathematical evaluation of *in* vitro drug release was performed using two diffusion models: Higuchi and Korsmeyer models.[24,25] The correlation coefficient (r^2) obtained by plotting the experimental data according to the equations of these models allowed the Higuchi model to be identified as the most appropriate:

$$Q_t = K_{\mathrm{H}} t_2^n \tag{8}$$

or Korsmeyer–Peppas:

$$\frac{M_t}{M_\infty} = K_{\mathrm{K}} t^n \tag{9}$$

where M_t/M_∞ represents the fractional drug release, K_{H} and K_{K} are the release constants for the Higuchi and Korsmeyer models, respectively, and n is the release

exponent defining the release mechanism. The Higuchi model describes the release of water-soluble or poorly water-soluble drugs from semi-solid or solid matrix systems.[24] Meanwhile, the exponent n, as defined by Peppas,[50] distinguishes different release mechanisms: Fickian diffusion occurs when $n = 0.5$ and is time-dependent, whereas non-Fickian diffusion is observed when n ranges between 0.5 and 1.0. Case II transport corresponds to $n = 1.0$, while super Case II transport occurs when $n > 1$. When $n < 0.5$, the diffusion mechanism is associated with the quasi-Fickian model. The results of the data analysis are summarised in Table IV.

TABLE IV. Coefficients of correlation and dissolution rate constants of Vals from microspheres in simulated intestinal fluid

Code	K_H	R^2	ln K_K	K_K	n	R^2
L1	0 .481	0.927	1.242	3.463	0.086	0.972
L2	0.344	0.973	0.864	2.373	0.050	0.993
L3	2.281	0.982	2.571	13.080	0.132	0.999
L4	1.592	0.969	2.478	11.917	0.013	0.929
L5	1.013	0.973	1.959	7.092	0.043	0.999
L6	2.045	0.968	2.733	15.379	0.011	0.986
L7	4.237	0.996	2.578	13.171	0.415	0.992
L8	3.708	0.983	2.746	15.580	0.301	0.977

The correlation coefficients and dissolution rate constants of valsartan released from microspheres, based on the investigated models in an intestinal medium, are summarised in Table IV. Overall, according to the coefficient of determination (R^2) values presented in Table IV, the Korsmeyer–Peppas model provided the best fit, with R^2 greater than 0.97 for all formulations except L1 in the Higuchi model ($R^2 = 0.927$) and L4 in the Korsmeyer–Peppas model ($R^2 = 0.929$). These strong correlations suggest that the drug release is predominantly governed by diffusion mechanisms.

The dissolution rate constants of the drug in the simulated intestinal medium (pH 7.4), derived from the Higuchi's equation plots, ranged from 4.237 $min^{-1/2}$ for L7; 3.708 $min^{-1/2}$ for L8; 2.281$min^{-1/2}$ for L3; 2.045 $min^{-1/2}$ for L6; 1.592 $min^{-1/2}$ for L4; 1.013 $min^{-1/2}$ for L5 ; 0.481 $min^{-1/2}$ for L1 to 0.344 min^{-1} for L2. These values, reflect relatively low dissolution constants in the intestinal medium (see Table IV) and are consistent with the results of previous experiments.

Furthermore, the lower n values (0.011–0.415) obtained from the Korsmeyer–Peppas equation (Table IV) suggest a quasi-Fickian release mechanism, ruling out matrix erosion or solubilisation as the dominant release processes.[25,47,48,50,51]

CONCLUSION

This study investigated the effect of valsartan microencapsulation on its release profile. A significant sustained release effect was observed when valsartan was encapsulated with CAB polymer, reaching up to 7.67 % in batch L2. Fur-

thermore, the influence of formulation parameters on the properties and *in vitro* release behaviour of valsartan-loaded CAB microspheres prepared by solvent--evaporation microencapsulation was evaluated. The results showed that increasing the stirring speed during microsphere preparation generally led to a reduction in microparticle size, but could also result in increased valsartan loss, thereby reducing the amount of encapsulated drug. In addition, the use of PVA produced spherical microspheres with smooth, porous surfaces, which facilitated controlled drug release. In contrast, the incorporation of Tween 80 resulted in irregularly shaped microspheres with rough surfaces and larger pores, which accelerated valsartan release. Finally, the inclusion of an additional matrix, such as PBS, resulted in the formation of particularly small microparticles, which were associated with more pronounced valsartan release. These findings highlight the importance of selecting formulation parameters and excipients to modulate the release characteristics of microspheres and optimise the efficacy of drug delivery systems.

In summary, the characteristics of the microspheres were strongly influenced by both the process and the formulation parameters. Higher stirring speeds reduced particle size and improved homogeneity, though they lowered drug loading. PVA produced smaller, smoother particles with a higher encapsulation efficiency than Tween 80 did. Using a lower D/C ratio further enhanced size uniformity and drug entrapment. Polymer properties such as molar mass and viscosity also modulated particle size and loading.

Acknowledgements. The authors would like to thank the General Directorate of Scientific Research and Technological Development (DGRSDT) and the Ministry of Higher Education and Scientific Research (MESRS) of Algeria for their invaluable support during the research.

И З В О Д

ОПТИМИЗАЦИЈА КОНТРОЛИСАНОГ ОСЛОБАЂАЊА ВАЛСАРТАНА ПРЕКО ЦЕЛУЛОЗНОГ АЦЕТАТА-БУТИРАТА И МИКРОСФЕРА ПОЛИ (БУТИЛЕН-СУКЦИНАТА): УТИЦАЈ УСЛОВА ФОРМУЛАЦИЈЕ

AISSA BOUHARAOUA[1], HAOUARIA MERINE[1] и YOUSSEF RAMLI[2]

[1]Laboratory of Macromolecular Physical and Organic Chemistry, Faculty of Exact Sciences, University of Djillali Liabes, Sidi Bel-Abbes, Algeria и [2]Laboratory of Medicinal Chemistry, Drug Sciences Research Center, Faculty of Medicine and Pharmacy, Mohammed V University, Rabat, Morocco

Ова студија истражује формулацију микросфера целулозног ацетата-бутирата (CAB) напуњених валсартаном, припремљених микроенкапсулацијом испаравањем растварача, како би се проценило њихово *ин витро* понашање ослобађања и утицај параметара формулације. Студија је испитала ефекте брзине мешања, стабилизатора и матричних материјала на величину честица и ослобађање лека. Повећање брзине мешања смањило је величину честица, али је такође довело до већег губитка валсартана, смањујући ефикасност енкапсулације. Коришћење сурфактанта полимлечна киселина резултирало је глатким, сферним и порозним микросферама које су побољшале контролисано ослобађање. Насупрот томе, коришћење Tween 80 довело је до неправилних честица са

грубим површинама и већим порама које су убрзале ослобађање лека. Укључивање поли(бутилен-сукцината) у матрицу резултирало је формирањем мањих микрочестица и значајно већом стопом ослобађања валсартана. Ови налази наглашавају важност оптимизације параметара формулације и помоћних материја за контролу карактеристика ослобађања лекова и побољшање перформанси система за испоруку лекова.

(Примљено 21. маја, ревидирано 15. Јула, прихваћено 10. септембра 2025)

REFERENCES

1. Y. D. Yan, J. H.Sung, K. K. Kim, D. W.Kim, J. O.Kim, B.-J.Lee, C. S.Yong, H.-G. Choi, *Int. J. Pharm.* **422** (2012) 202 (https://doi.org/10.1016/j.ijpharm.2011.10.053)
2. O. Sadoun, F. Rezgui, C. G'Sell, *Mat. Sci. Eng., C* **90** (2018) 189 (https://doi.org/10.1016/j.msec.2018.04.041)
3. M. C Michel, H. R Brunner, C. Fosterd, Y. Huo, *Pharm. Ther.* **164** (2016) 1 (https://doi.org/10.1016/j.pharmthera.2016.03.019)
4. Z. Ma, Z. Fu, N. Li, S. Huang, L. Chi, *BMJ Open* **14** (2024) e088744 (https://doi.org/10.1136/bmjopen-2024-088744)
5. N. Siddiqui, A. Husain, L. Chaudhry, M.S. Alam, M. Mitra, P.S. Bhasin, *J. App. Pharm. Sci.* **01** (2011) 12 (https://japsonline.com/admin/php/uploads/54_pdf.pdf)
6. J.-B Park, C. Park, Z. Z. Piao, H. H. Amin, N. M. Meghani, P. H. L. Tran, T. T. D. Tran, J.-H Cui, Q.-R. Cao, E. Oh, B.-J. Lee, *J. Drug Delivery Sci. Techn.* **46** (2018) 365 (https://doi.org/10.1016/j.jddst.2018.05.031)
7. K. P. Dwivedi, S. Jaiswal, A. K. Srivastava, S. K., Tiwari, P. Singh, S. maddhesiya, N. K. Verma, *Int. J. Med. Pharm. Res.* **4** (2023) 76 (https://doi.org/10.5281/zenodo.8201865)
8. B. Cappello, C. di Maio, M. Iervolino, A. Miro, *J. Incl. Phenom. Macrocycl. Chem.* **54** (2006) 289 (https://doi.org/10.1007/s10847-005-9004-y)
9. C. E. De Matos Jensen, R. A. S. Dos Santos, A. M. L. Denadai, C. F. F. Santos, A. N. G. Braga, R. D. Sinisterra, *Molecules* **15** (2010) 4067 (https://doi.org/10.3390/molecules15064067)
10. B. N. Nalluri, K. P. R. Chowdary, K. V. R. Murthy, G. Becket, P. A. Crooks, *AAPS PharmSciTech **8*** (2007) E1 (https://doi.org/10.1208/pt0802036)
11. B. Parmar, S. Mandal, K. C. Petkar, L. D. Patel, K. K. Sawant, *Int. J. Pharm. Sci. Nanotechol*. **4** (2011)1483 (https://doi.org/10.1016/j.ijpharm.2010.09.007)
12. D. X. Li, Y. D. Yan, D. Hoon Oh, K. Y. Yang, Y. G. Seo, J. O. Kim, Y. I. Kim, C. S. Yong, H. G. Choi, *Drug Deliv.* **17** (2010) 322 (https://doi.org/10.3109/10717541003717031)
13. G. Verreck, I. Chun, J. Peeters, J. Rosenblatt, M. E Brewster, *Pharm. Res.* **20** (2003)10 (https://doi.org/10.1023/a:1023450006281)
14. E. Hajba-Horváth, A. Fodor-Kardos, N. Shah, G. M. Wacker, T. Feczkó, *Int. J. Mol. Sci.* **22** (2021) 13069 (https://doi.org/10.3390/ijms222313069)
15. , *Handbook of Pharmaceutical Excipients*, 5th ed., R. C. Rowe, P. J. Sheskey, S. C. Owen, Eds., American Pharmacists Association, Washington, DC, 2006
16. T. Mahmood, R. M. Sarfraz, A. Ismail, M. Ali, A. Khan, *ASSAY Drug Dev. Technol*. **21** (2023) 65 (https://doi.org/10.1089/adt.2022.119)
17. O. C. Larbi, H. Merine, Y. Ramli, F. B. Toumi, K. Guemra, A. Dehbi, *J. Serb. Chem. Soc.* **83** (2018) 1243 (https://doi.org/10.2298/JSC171112065L)

18. K. Badis, H. Merine, Y. Ramli, O. C. Larbi, C. H. Memou, *J. Mexican Chem. Soc.* **66** (2022) 17 (https://doi.org/10.29356/jmcs.v66i1.1583)
19. S. Chirani, M.O. Lebig, S. Bouameur, M. Mouffok, N. Chirani, N. Chafi, K. Guemra, *Indian J. Pharm. Educ. Res.* **51** (2017) 79 (https://doi.org/10.5530/ijper.50.4.21)
20. K. Kaczmarski, J. C. Bellot, *Acta Chromatogr.* **13** (2003) 22 (https://www.researchgate.net/publication/237326465)
21. C. Jégat, J. L. Taverdet, *Polym. Bull.* **44** (2000) 345 (https://doi.org/10.1007/s002890050612)
22. J. G. Wagner, *J. Pharm. Sci.* **58** (1969) 1253 (https://doi.org/10.1002/jps.2600581021)
23. M. Gibaldi, S. Feldman, *J. Pharm. Sci.* **56** (1967) 1238 (https://doi.org/10.1002/jps.2600561005)
24. T. Higuchi, *J. Pharm. Sci.* **52** (1963) 1145 (https://doi.org/10.1002/jps.2600521210)
25. R. W. Korsmeyer, R. Gurny, E. Doelker, P. Buri, N. A. Peppas, *Int. J. Pharm.* **15** (1983) 25 (https://doi.org/10.1016/0378-5173(83)90064-9)
26. A. André-Abrant, J. L. Taverdet, J. Jay, *Eur. Polym. J.* **37** (2001) 955 (https://doi.org/10.1016/S0014-3057(00)00197-X)
27. E. Schlicher, N. S. Postma, J. Zuidema, H. Talsma, W. Hennink, *Int. J. Pharm.* **153** (1997) 235 (https://doi.org/10.1016/S0378-5173(97)00116-6)
28. C. Prieto, Z. Evtoski, M.Pardo-Figuerez, J. Hrakovsky, J. M. Lagaron, Mol. Pharmaceutics **18** (2021) 2947 (https://doi.org/10.1021/acs.molpharmaceut.1c00098)
29. J.O. Hinze, *AIChE J.* **1** (1955) 289 (https://doi.org/10.1002/aic.690010303)
30. M. Mouffok, A. Mesli, I. Abdelmalek, E. Gontier, *J. Serb. Chem. Soc.* **81** (2016) 1183 (https://doi.org/10.2298/JSC160308068M)
31. A. Merdoud, M. Mouffok, A. Mesli, N. Chafi, M. Chaib, *J. Serb. Chem. Soc.* **85** (2020) 531 (https://doi.org/10.2298/JSC190326132M)
32. P. Sansdrap, A. J. Moes, *Int. J. Pharm*. **98** (1993) 157 (https://doi.org/10.1016/0378-5173(93)90052-H)
33. R. Brahmi, K. Diaf, Z. ELBahri, M. Baitiche, *J. Serb. Chem. Soc.* **89** (2024) 91 (https://doi.org/10.2298/JSC230501088B)
34. C. Grandfils, P. Flandroy, N. Nihant, S. Barbette, R. Jerome, P. Teyssie, A. Thibaut, *J. Biomed. Mater. Res.* **26** (1992) 467 (https://doi.org/10.1002/jbm.820260405)
35. R. Jeyanthi, R. C. Mehta, B. C. Thanoo, P. P. De Luca, *J. Microencapsul.* **14** (1997) 163 (https://doi.org/10.3109/02652049709015330)
36. W. I. Li, K. W. Anderson, P. P. Deluca, *J. Cont. Rel.* **37** (1995) 187 (https://doi.org/10.1016/0168-3659(95)00077-1)
37. Q. Yang, G. Owusu-Ababio, *Drug Dev. Ind. Pharm.* **26** (2000) 61 (https://doi.org/10.1081/DDC-100100328)
38. S. Mao, Y. Shi, L. Li, J. Xu, A. Schaper, T. Kissel, *Eur. J. Pharm. Biopharm.* **68** (2008) 214 (https://doi.org/10.1016/j.ejpb.2007.06.008)
39. B. K. Kim, S. J. Hwang, J. B. Park, H. J. Park, *J. Microencapsul*. **22** (2005) 193 (https://doi.org/10.1080/02652040400015346)
40. M. A. Benoit, B. Baras, J. Gillbard, *Int. J. Pharm.* **184** (1999) 73 (https://doi.org/10.1016/s0378-5173(99)00109-x)
41. P. Le Corre, P. Le Guevello, V. Gajan, F. Chevanne, R. Le Verge, *Int. J. Pharm*. **107** (1994) 41 (https://doi.org/10.1016/0378-5173(94)90300-X)

42. J.C. Jeong, J. Lee, K. Cho, *J. Control. Rel.* **92** (2003) 249 (https://doi.org/10.1016/S0168-3659(03)00367-5)
43. C. Y. Yang, S. Y. Tsay, R. C. C. Tsiang, *J. Microencapsul.* **17** (2000) 269 (https://doi.org/10.1080/026520400288256)
44. M. S. Islas, C. A. Franca, S. B. Etcheverry, E. G. Ferrer, P. A. M. Williams, *Vib. Spectrosc*. **62** (2012) 143 (https://doi.org/10.1016/j.vibspec.2012.04.009)
45. L. Wang, C. Du, Y. Yang, P. Zhang, S. Yuan, *Molecules* **29 (**2024) 5467 (https://doi.org/10.3390/molecules29225467)
46. Y.-S. Youn, J. H. Oh, K. H. Ahn, M. Kim, J. Kim, Y.-W. Lee, *J. Supercrit. Fluids* **59** (2011) 117 (https://doi.org/10.1016/j.supflu.2011.07.008)
47. G. Flesch, P. Muller, P. Lloyd, *Eur. J. Clin. Pharmcol*. **52** (1997) 115 (https://doi.org/10.1007/s002280050259)
48. M. Saydam, S. Takkaj, *FABAD J. Pharm. Sci.* **32** (2007) 185 (https://www.dergi.fabad.org.tr/pdf/volum32/issue4/185-196.pdf)
49. S. Milovanovic, J. Djuris, A. Dapčević, M. L. Skoric, D. Medarevic, S. M. Pavlovic, S. Ibric, *J. Polym. Res.* **28** (2021) 74 (https://doi.org/10.1007/s10965-021-02440-1)
50. P. L. Ritger, N. A. Peppas, *J. Control. Rel.* **5** (1987) 37 (http://dx.doi.org/10.1016/0168-3659(87)90034-4)
51. K. S. Soppimath, A. R. Kulkarni, T. M. Aminabhavi, *J. Microencapsulation* **18** (2001) 397 (https://doi.org/10.1080/02652040010018083).